ChannelGAN: Deep Learning-Based Channel Modeling and Generating

Han Xiao, Wenqiang Tian, Wendong Liu, and Jia Shen

***Abstract*—The increasing complexity on channel modeling and the cost on collecting plenty of high-quality wireless channel data have become the main bottlenecks of developing deep learning (DL) based wireless communications. In this letter, a DL-based channel modeling and generating approach namely ChannelGAN is proposed. Specifically, the ChannelGAN is designed on a small set of 3rd generation partnerships project (3GPP) link-level multiple-input multiple-output (MIMO) channel. Moreover, two evaluation mechanisms including i) power comparison from the perspective of delay and antenna domain and ii) cross validation are implemented where the power comparison proves the consistency between the modeled fake channel and real channel, and the cross validation verifies the effectiveness and availability of the generated fake channel for supporting related DL-based channel state information (CSI) feedback.**

***Index Terms*—Channel modeling and generating, deep learning, generative adversarial network, CSI feedback.**

I. Introduction

AS THE basis of wireless communication system design and performance evaluation, channel modeling has attracted lots of attentions in the 6th generation (6G) pre-research. However, considering the increasing complexity of wireless environments, the extension of frequency band and the introduction of large-scale multiple-input multiple-output (MIMO) systems, current channel modeling schemes are difficult extracting the complicated wireless characteristics effectively. Therefore, more efficient channel modeling alternatives require further studies.

Recently, deep learning (DL) based wireless communication has been regarded as a potential technology in the 6G [1]–[4]. In addition to accurate channel modeling, DL-based wireless communication approaches also require amounts of high-quality wireless channel dataset to support the training of neural network (NN). However, the collection of large wireless channel data is quite costly and time-consuming, which motivates novel channel data generating solutions to support the training of NN. As pioneer works, the generative adversarial network (GAN) [5] based channel modeling methods are introduced to model the additive white gaussian noise (AWGN) [6] and multi-path single-input single-output (SISO) [7] channels, respectively. However, some pivotal realistic factors should be further investigated. Firstly, considering the difficulty of acquisition of extensive real channel data, the scale of real channel data used for training the GAN should be limited. Secondly, a more complex and practical scenario instead of AWGN or SISO channel requires further studied. Thirdly, the effective evaluation methodology also needs to be established.

In this letter, a novel approach referred to as ChannelGAN is proposed for channel modeling and generating. Specifically, the ChannelGAN is designed on a small set of link-level MIMO channel defined in the 3rd generation partnerships project (3GPP). Moreover, two evaluation mechanisms including i) power comparison from the perspective of delay and antenna domain and ii) cross validation are implemented where the power comparison proves the consistency between the modeled fake channel and real channel, and the cross validation verifies the effectiveness and availability of the generated fake channel for supporting related DL-based channel state information (CSI) feedback [1].

II. System Description

The clustered delay line (CDL) MIMO channel model is considered in this letter, which is widely utilized for link-level performance evaluation in 3GPP TR38.901 [8]. Specifically, five types of CDL channel models, referred to as CDL-A to CDL-E are recommended, where CDL-A, CDL-B and CDL-C represent the non-line-of-sight (NLOS) channels, while CDL-D and CDL-E are provided for line-of-sight (LOS) counterparts. Generally, different delays, powers, angle of departures, angle of arrivals and other parameters are involved to characterize various CDL channel models. For simplicity, the original CDL channel is denoted as the *real channel*. In comparison, the modeled and generated channel is defined as the *fake channel*. Note that the CDL channel models are only used for elaborating our proposed scheme, which can be naturally extended to more complicated channel conditions.

We consider a typical MIMO system with N_{t} transmit antennas at base station (BS) and N_{r} receive antennas at user equipment (UE). Thus the real channel in time domain with one orthogonal frequency division multiplexing (OFDM) symbol can be denoted as $\widetilde{\mathbf{H}} \in \mathbb{C}^{N_{\mathrm{t}} \times N_{\mathrm{r}} \times N_{\mathrm{d}}}$, where N_{d} represents the number of delay paths. Moreover, we further reformulate the real channel as $\mathbf{H} \in \mathbb{R}^{N_{\mathrm{a}} \times N_{\mathrm{d}} \times 2}$ with normalized element amplitude in $[-1, 1]$, where $N_{\mathrm{a}} = N_{\mathrm{t}} N_{\mathrm{r}}$ denotes the number of antenna pairs, and the last dimension with value of 2 represents the real and imaginary parts of original complex channel, respectively. Denotes $\tilde{p}_{\mathrm{r}}$ as the actual distribution of $\mathbf{H}$, which is very difficult to obtain since it theoretically requires infinite real channel data. Generally, the procedure of channel modeling can be illustrated as finding a fake channel, whose generated distribution p_{f} is aimed at matching the real channel distribution $\tilde{p}_{\mathrm{r}}$. It can be formulated as

$$\min_{p_{\mathrm{f}}} L(\tilde{p}_{\mathrm{r}}, p_{\mathrm{f}}), \tag{1}$$

where $L(\cdot, \cdot)$ represents a function that measures the distance between two input distributions, e.g., Kullback-Leibler divergence, Jensen-Shannon divergence and earth-mover (EM) distance. However, as the wireless channel becomes more

Manuscript received December 13, 2021; accepted December 30, 2021. Date of publication January 4, 2022; date of current version March 9, 2022. The associate editor coordinating the review of this article and approving it for publication was D. B. da Costa. *(Corresponding author: Wenqiang Tian.)*

The authors are with the Department of Standards Research, OPPO, Beijing 100000, China (e-mail: xiaohan1@oppo.com; tianwenqiang@oppo.com; liuwendong1@oppo.com; sj@oppo.com).

Digital Object Identifier 10.1109/LWC.2021.3140102

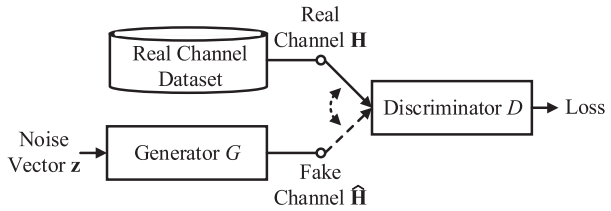

Fig. 1. Framework of proposed ChannelGAN.

and more complex, it is extremely difficult for existing mathematical channel modeling methods to interpret the real channel distribution $\tilde{p}_{\mathrm{r}}$, which brings challenges to solving (1).

III. Proposed ChannelGAN

A. Framework of ChannelGAN

Since the actual distribution $\tilde{p}_{\mathrm{r}}$ is difficult to acquire, a small real channel dataset $\mathcal{H} = \{\mathbf{H}|\mathbf{H} \sim p_{\mathrm{r}}\}$ is utilized with distribution p_{r}. Generally, with relatively uniform channel data sampling, the real channel dataset could get more representative of realistic channel distributions with $p_{\mathrm{r}} \to \tilde{p}_{\mathrm{r}}$. Considering that a small cardinality of $\mathcal{H}$ namely $|\mathcal{H}|$ indicates insufficient channel samples, which may be not enough to train a NN effectively, a DL-based solution described in Fig. 1, named as ChannelGAN, is proposed to model the distribution p_{r} and generate a fake channel dataset $\widehat{\mathcal{H}} = \{\widehat{\mathbf{H}}|\widehat{\mathbf{H}} \sim p_{\mathrm{f}}\}$ with $|\widehat{\mathcal{H}}| \gg |\mathcal{H}|$. Hence the optimization problem (1) can be approximated as

$$\min_{p_{\mathrm{f}}} L(p_{\mathrm{r}}, p_{\mathrm{f}}). \tag{2}$$

To stably implement on complex channel data, the Wasserstein GAN with gradient penalty (WGAN-GP) which utilizes EM distance is selected as the backbone of ChannelGAN due to its stability during training phase [9]. If two distributions are interpreted as two different ways of piling up a certain amount of dirt, the EM distance is informally defined as the minimum cost of turning one pile into the other, where the cost is the amount of dirt moved times the distance by which it is moved. By adapting EM distance as $L(\cdot,\cdot)$. we have

$$\begin{aligned} L(p_{\mathrm{r}}, p_{\mathrm{f}}) &= \inf_{\psi \in \Psi(p_{\mathrm{r}}, p_{\mathrm{f}})} \mathbb{E}_{(\mathbf{H},\widehat{\mathbf{H}})\sim\psi}[\|\mathbf{H}-\widehat{\mathbf{H}}\|_{\mathrm{F}}] \\ &\overset{(a)}{=} \sup_{f \in \mathcal{Z}} \mathbb{E}_{\mathbf{H}\sim p_{\mathrm{r}}}[f(\mathbf{H})] - \mathbb{E}_{\widehat{\mathbf{H}}\sim p_{\mathrm{f}}}[f(\widehat{\mathbf{H}})], \end{aligned} \tag{3}$$

in which $\Psi(p_{\mathrm{r}}, p_{\mathrm{f}})$ denotes the set of all possible joint distributions with marginals of p_{r} and p_{f}, $\|\cdot\|_{\mathrm{F}}$ denotes the Frobenius norm, $\mathcal{Z}$ denotes the set of 1-Lipschitz functions, and (a) holds according to Kantorovich-Rubinstein duality [10]. In order to formulate the EM distance, i.e., find the supremum in (3), a discriminator NN D is introduced to learn a 1-Lipschitz function $f(\cdot)$ which has mild gradient and can improve the stability of training. Meanwhile, a generator NN G is constructed to map a noise vector $\mathbf{z}$ sampled with gaussian distribution p_{z} to the generated fake channel with $\widehat{\mathbf{H}} \sim p_{\mathrm{f}}$, which is trained to minimize the EM distance between p_{r} and p_{f} namely the minimum of (3). Thus, the objective (3) can be rewritten as

$$\begin{aligned} &\min_{G} \max_{D\in\mathcal{Z}} \mathbb{E}_{\mathbf{H}\sim p_{\mathrm{r}}}[D(\mathbf{H})] - \mathbb{E}_{\widehat{\mathbf{H}}\sim p_{\mathrm{f}}}[D(\widehat{\mathbf{H}})] \\ &= \min_{G} \max_{D\in\mathcal{Z}} \mathbb{E}_{\mathbf{H}\sim p_{\mathrm{r}}}[D(\mathbf{H})] - \mathbb{E}_{\mathbf{z}\sim p_{\mathrm{z}}}[D(G(\mathbf{z}))], \end{aligned} \tag{4}$$

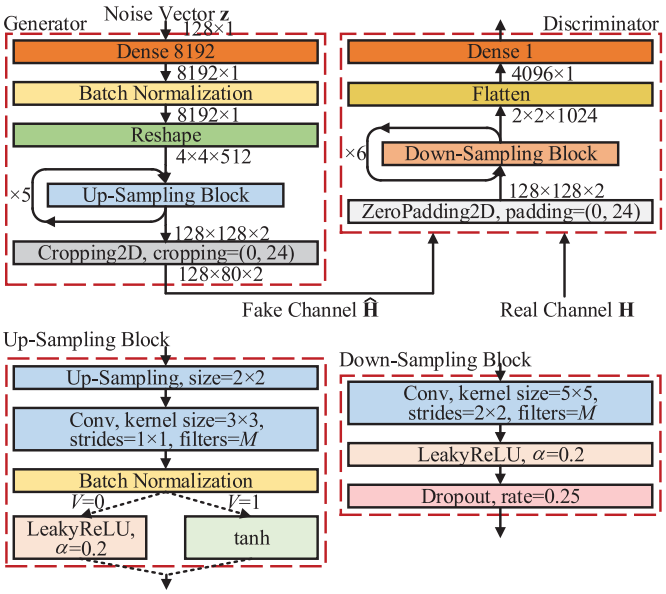

Fig. 2. Structure of proposed ChannelGAN.

where $\widehat{\mathbf{H}} = G(\mathbf{z})$. Furthermore, the gradient penalty is added to enforce the Lipschitz constrain ensuring stable training, resulting in the following minimax objective which can be regarded as the joint loss for ChannelGAN [9],

$$\begin{aligned} &\min_{G} \max_{D} \mathbb{E}_{\mathbf{H}\sim p_{\mathrm{r}}}[D(\mathbf{H})] - \mathbb{E}_{\mathbf{z}\sim p_{\mathrm{z}}}[D(G(\mathbf{z}))] \\ &\quad -\lambda \mathbb{E}_{\bar{\mathbf{H}}\sim p_{\mathrm{s}}}[(||\nabla_{\bar{\mathbf{H}}} D(\bar{\mathbf{H}})||_2 - 1)^2], \end{aligned} \tag{5}$$

where $\lambda > 0$, $\bar{\mathbf{H}} = \epsilon\mathbf{H} + (1-\epsilon)G(\mathbf{z})$ and ϵ is sampled from a uniform distribution $u[0, 1]$. During training phase, ChannelGAN alternately optimizes the generator G and the discriminator D in competition with each other, i.e., iteratively and alternately solving the max and min optimization problems in (5) where the EM distance between the distributions of fake channel p_{f} and real channel p_{r} is gradually decreased at the same time. When the ChannelGAN arrives convergence with matched p_{f} and p_{r}, the generator G can be regarded as a stable storage of channel model and used to generate the fake channel data to form a extensive training dataset to support related DL-based wireless communication tasks.

B. Structure of ChannelGAN

The structure of the proposed ChannelGAN is illustrated in Fig. 2. In order to better process large-size MIMO channel tensor and extract complex features, the structure of ChannelGAN considers wide dense layer and deep convolutional layer introduced as follows.

For the generator G, it maps a noise vector $\mathbf{z}$ to a fake channel $\widehat{\mathbf{H}} \in \mathbb{R}^{N_{\mathrm{a}} \times N_{\mathrm{d}} \times 2}$. Firstly, in order to convert from input noise vector to the feature maps, the noise vector $\mathbf{z}$ is firstly processed by a dense layer along with batch normalization and reshape. Next, five up-sampling blocks are stacked up. Specifically, each up-sampling block is composed of a 2×2 up-sampling layer (nearest neighbor interpolation), a 3×3 convolutional layer (Conv) with M filters and a batch normalization layer. Two optional activation functions are also attached at the tail of each block with the opting flag $V \in \{0, 1\}$, where $V = 0$ and $V = 1$ indicate utilization of leaky rectified linear unit (LeakyReLU) and hyperbolic tangent

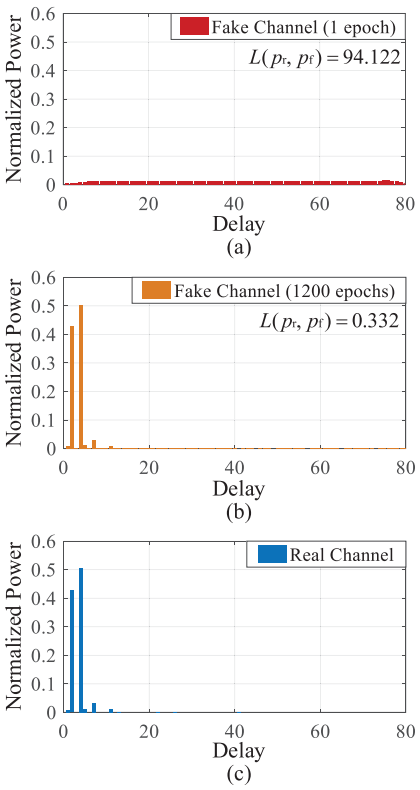

Fig. 3. Comparison of the delay-power spectrum (averaging 1000 samples): (a) fake channel trained for 1 epoch, (b) fake channel trained for 1200 epochs and (c) real channel.

function (tanh), respectively. Here five up-sampling blocks are configured with parameters $M = \{1024, 512, 256, 128, 2\}$ and $V = \{0, 0, 0, 0, 1\}$ sequentially. Note that the tanh in the last Up-Sampling Block limits the amplitude of the elements in fake channel in $[-1, 1]$ which matchs the real channel, and the LeakyReLu in remaining blocks brings the non-linear transformation to the network. Finally, the two-dimensional cropping layer (Cropping2D) is used to maintain the shape of generated fake channel $\widehat{\mathbf{H}}$ consistent with the real channel $\mathbf{H}$.

For the discriminator D, the input is firstly padded by a two-dimensional zero padding layer (ZeroPadding2D). Then, six down-sampling blocks are stacked up, where the 5×5 Conv with the strides of 2×2 and $M = \{32, 64, 128, 256, 512, 1024\}$ filters, a LeakyReLU and a dropout layer are deployed sequentially. In the end, a flatten operation and dense layer with single output are utilized.

IV. Simulation Results

In this section, some simulation results are presented to verify the consistency between the modeled fake channel and the real channel. Meanwhile, the effectiveness and availability of the generated fake channel is also proved through the cross validation on DL-based CSI feedback [1]. The basic simulation parameters are shown in Table I. Specifically, the CDL-C channel model is considered to illustrate our proposal [8].

A. Comparison of Real and Fake Channel

The normalized power comparisons between fake channels at initial state after 1 epoch, convergent state after 1200 epochs and the real channel have been visualized from the perspective of delay domain, antenna domain and three-dimension views

TABLE I
Basic Simulation Parameters

Parameter	Value
System bandwidth	10MHz
Carrier frequency	3.5GHz
Subcarrier spacing	15KHz
RB number N_{RB}	48
Subband number N_{sb}	12
RBs per subband	4
Tx antennas N_{t}	32
Rx antennas N_{r}	4
Delay paths N_{d}	80
Channel model	CDL-C
UE speed	3km/h
Delay spread	300ns
Modulation Coding Scheme [11]	19
Optimizer	Adam
Learning rate for ChannelGAN	0.0002

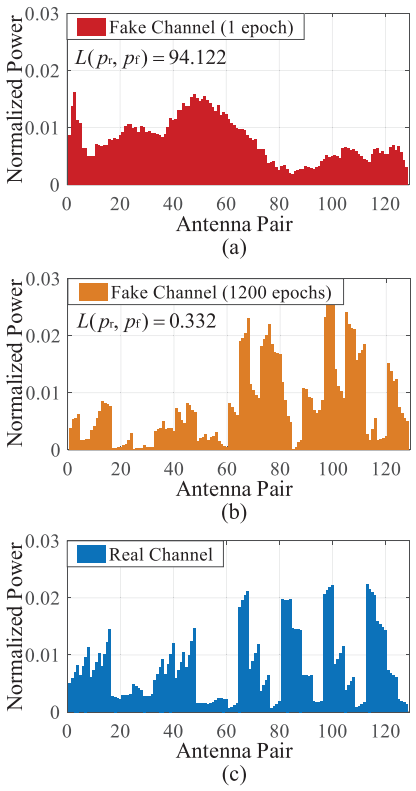

Fig. 4. Comparison of the power distribution (1 sample) across antennas pairs of the 4th delay path: (a) fake channel trained for 1 epoch, (b) fake channel trained for 1200 epochs and (c) real channel.

in Fig. 3, 4 and 5, respectively. A small set of 2000 real channel samples is utilized to train the ChannelGAN, where the EM distance $L(p_{\mathrm{r}}, p_{\mathrm{f}})$ decreases from 94.122 to 0.332 after 1200 epochs. Note that the smaller the EM distance $L(p_{\mathrm{r}}, p_{\mathrm{f}})$, the more similar the distributions p_{r} and p_{f}, the better the fit of features of fake channel $\widehat{\mathbf{H}} \sim p_{\mathrm{f}}$ to the real channel $\mathbf{H} \sim p_{\mathrm{r}}$, and the better the modeling performance of ChannelGAN. It can be clearly observed that compared to the initial state of (a) in each figure, the power distribution of convergent state in (b) is more consistent to real channel counterpart from both the delay and antenna domain.

More specifically, the comparison of delay-power spectrum in Fig. 3 are obtained by averaging 1000 samples, so that the

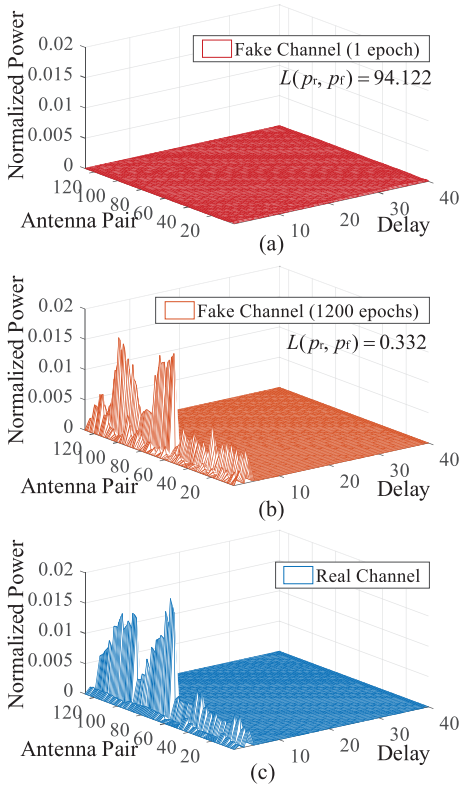

Fig. 5. Three-view visualization comparison (1 sample): (a) fake channel trained for 1 epoch, (b) fake channel trained for 1200 epochs and (c) real channel.

statistical characteristics of the generated fake channel and real CDL-C channel model in delay domain can be clearly revealed. Obviously, the 2nd and 4th delay paths are dominant with remarkable powers, while the remaining paths are relatively slight. Observed from Fig. 3 (b) and (c), besides accurate modeling on the 2nd and 4th delay paths in terms of normalized power distribution, the characteristics of several slighter paths, such as the 1st, 5th, 7th and 11th counterparts, are also well imitated at the convergent state. In addition, the comparison of normalized power distribution of the 4th delay path for one sample in antenna domain is depicted in Fig. 4. Apparently, considering $N_{\mathrm{t}} = 32$ and $N_{\mathrm{r}} = 4$ antennas are deployed, the normalization power distributions are regularly varied every 4 indices within antenna pair dimension in both Fig. 4 (b) for fake channel at convergent state of ChannelGAN and Fig. 4 (c) for real channel. Fig. 5 provides the visualizations of channel features in three-dimension views, where the distribution characteristics of the real channel are also well modeled through proposed ChannelGAN at convergent state.

B. Cross Validation on DL-Based CSI Feedback

To verify the effectiveness and availability of generated fake channel using ChannelGAN, the cross validation on the DL-based CSI feedback is introduced, where the eigenvector based CSI feedback mechanism, referred to as EVCsiNet is utilized [1]. In preprocessing, the frequency domain channel can be calculated using $N_{\mathrm{FFT}} = 1024$ points fast Fourier transform (FFT) based on the time domain channel. Next, the eigenvectors for $N_{\mathrm{sb}} = 12$ subbands within 48 resource blocks (RBs) could be obtained using eigenvalue decomposition. Hence, the joint eigenvector can be denoted as $\mathbf{W} = [\mathbf{w}_1, \ldots, \mathbf{w}_{N_{\mathrm{sb}}}] \in \mathbb{C}^{N_{\mathrm{t}} \times N_{\mathrm{sb}}}$, which are then compressed and recovered through EVCsiNet [1] with number of feedback bits $B = 48$.

TABLE II
ρ COMPARISON IN POSITIVE VALIDATION

N_{s}	$\rho(\mathcal{W}_{\mathrm{r}}, A_{\mathrm{r}}(\mathcal{W}_{\mathrm{r}}))$	$\rho(\mathcal{W}_{\mathrm{f}}, A_{\mathrm{r}}(\mathcal{W}_{\mathrm{f}}))$
20000	0.885	0.864
2000	0.778	0.758
1000	0.712	0.693
500	0.616	0.624
200	0.098	0.076

For simplicity, the corresponding eigenvector CSI set $\mathcal{W}$ obtained from real channel and fake channel are denoted as $\mathcal{W}_{\mathrm{r}}$ and $\mathcal{W}_{\mathrm{f}}$, respectively. Meanwhile, the corresponding EVCsiNet models $A(\cdot)$ trained on real CSI set $\mathcal{W}_{\mathrm{r}}$ and fake CSI set $\mathcal{W}_{\mathrm{f}}$ are denoted as $A_{\mathrm{r}}(\cdot)$ and $A_{\mathrm{f}}(\cdot)$, respectively. Usually, the average squared generalized cosine similarity (GCS) is utilized to evaluate the CSI compression and recovery accuracy as follows

$$\rho(\mathcal{W}, \mathcal{W}') = \frac{1}{|\mathcal{W}| N_{\mathrm{sb}}} \sum_{i=1}^{|\mathcal{W}|} \sum_{k=1}^{N_{\mathrm{sb}}} \left(\frac{\|\mathbf{w}_{k,i}^{\mathsf{H}} \mathbf{w}'_{k,i}\|_2}{\|\mathbf{w}_{k,i}\|_2 \|\mathbf{w}'_{k,i}\|_2} \right)^2, \quad (6)$$

where $\rho(\mathcal{W}, \mathcal{W}') \in [0, 1]$, $\mathcal{W}' = A(\mathcal{W}) = \{A(\mathbf{W}) | \mathbf{W} \in \mathcal{W}\}$ represents the predicted eigenvector CSI set with EVCsiNet $A(\cdot)$, $|\cdot|$ denotes the cardinality of a set, $\|\cdot\|_2$ denotes the ℓ_2 norm, $\mathbf{w}_{k,i}$ and $\mathbf{w}'_{k,i}$ represent the kth eigenvectors of ith sample in $\mathcal{W}$ and $\mathcal{W}'$, respectively. The higher the GCS performance, the higher the CSI compression and recovery accuracy.

1) Positive Validation: In order to investigate the effectiveness of generated fake channel, the positive validation is performed on DL-based CSI feedback. Specifically, an EVCsiNet $A_{\mathrm{r}}(\cdot)$ is trained on real CSI set with N_{s} samples. The ρ performance comparison between $\rho(\mathcal{W}_{\mathrm{r}}, A_{\mathrm{r}}(\mathcal{W}_{\mathrm{r}}))$ of testing on 1000 real CSI samples and $\rho(\mathcal{W}_{\mathrm{f}}, A_{\mathrm{r}}(\mathcal{W}_{\mathrm{f}}))$ of testing on 1000 fake CSI samples, is listed in Table II. Specifically, the 1000 fake CSI samples are obtained from $\widehat{\mathcal{H}}$ with $|\widehat{\mathcal{H}}| = 1000$, which is generated by the ChannelGAN trained on $|\mathcal{H}| = 2500$ real channel samples. It can be noticed that the performance gap between $\rho(\mathcal{W}_{\mathrm{r}}, A_{\mathrm{r}}(\mathcal{W}_{\mathrm{r}}))$ and $\rho(\mathcal{W}_{\mathrm{f}}, A_{\mathrm{r}}(\mathcal{W}_{\mathrm{f}}))$ is only about 3%, which reveals that the EVCsiNet trained on real CSI set is also appropriate for testing the fake CSI set and indicates the feature of true and false CSI in test set are very similar. Moreover, the best $\rho(\mathcal{W}_{\mathrm{f}}, A_{\mathrm{r}}(\mathcal{W}_{\mathrm{f}}))$ is up to 0.864 revealing that the features of fake CSI are similar to the true CSI in the training set. These demonstrate the real channel is well modeled by ChannelGAN and the effectiveness of generated fake channel.

2) Negative Validation: Besides the positive validation, in order to study the availability of generated fake channel and its performance on supporting training related DL-based wireless communication tasks, the negative validation based on EVCsiNet is also introduced. Firstly, similar to positive validation, an EVCsiNet $A_{\mathrm{r}}(\cdot)$ trained on a small real CSI set obtained from the corresponding real channel set $\mathcal{H}$ with $|\mathcal{H}| = N_{\mathrm{s}}$ real channel samples is tested on 1000 real CSI samples. Secondly, a ChannelGAN is trained using the same small set $\mathcal{H}$ to generate a fake channel set $\widehat{\mathcal{H}}$ with $|\widehat{\mathcal{H}}| = 20000$ samples. As comparison, another EVCsiNet $A_{\mathrm{f}}(\cdot)$ is trained on the fake CSI set $\mathcal{W}_{\mathrm{f}}$ processed from its corresponding

TABLE III
ρ COMPARISON IN NEGATIVE VALIDATION

N_{s}	$\rho(\mathcal{W}_{\mathrm{r}}, A_{\mathrm{r}}(\mathcal{W}_{\mathrm{r}}))$[1]	$\rho(\mathcal{W}_{\mathrm{r}}, A_{\mathrm{f}}(\mathcal{W}_{\mathrm{r}}))$
20000	0.885	/
2000	0.778	**0.874**
1000	0.712	**0.840**
500	0.616	**0.811**
200	0.098	**0.640**

[1] The performance of traditional codebook based method eTypeII $T_{\mathrm{II}}(\cdot)$ with $B = 49$ tested on real channel is $\rho(\mathcal{W}_r, T_{\mathrm{II}}(\mathcal{W}_{\mathrm{r}})) = 0.785$.

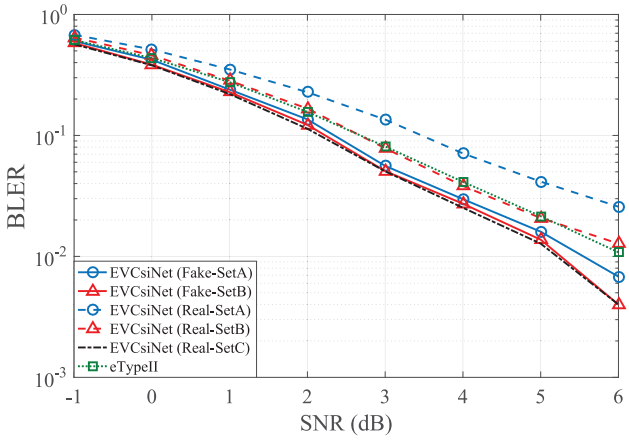

Fig. 6. Comparison of link-level BLER performance for the EVCsiNet trained on different datasets.

$\widehat{\mathcal{H}}$ and then tested on the same 1000 real CSI samples. As listed in Table III, the above two testings can be denoted as $\rho(\mathcal{W}_{\mathrm{r}}, A_{\mathrm{r}}(\mathcal{W}_{\mathrm{r}}))$ and $\rho(\mathcal{W}_{\mathrm{r}}, A_{\mathrm{f}}(\mathcal{W}_{\mathrm{r}}))$, respectively. It can be noticed that the significant performance improvement can be acquired from $\rho(\mathcal{W}_{\mathrm{r}}, A_{\mathrm{r}}(\mathcal{W}_{\mathrm{r}}))$ to $\rho(\mathcal{W}_{\mathrm{r}}, A_{\mathrm{f}}(\mathcal{W}_{\mathrm{r}}))$ with the same N_{s}. Especially in the case of using extremely small set with $N_{\mathrm{s}} = 200$, the performance gain reaches 553%. Moreover, the performance of EVCsiNet trained on 20000 real CSI samples and tested on 1000 real CSI samples is $\rho(\mathcal{W}_{\mathrm{r}}, A_{\mathrm{r}}(\mathcal{W}_{\mathrm{r}})) = 0.885$, which can be regarded as the upper bound of $\rho(\mathcal{W}_{\mathrm{r}}, A_{\mathrm{f}}(\mathcal{W}_{\mathrm{r}}))$. While by using ChannelGAN, we can achieve $\rho(\mathcal{W}_{\mathrm{r}}, A_{\mathrm{f}}(\mathcal{W}_{\mathrm{r}})) = 0.874$ based on only 2000 real channel samples. In summary, the negative validation demonstrates the availability of the generated fake channel on supporting training task and hence the superiority of our proposed ChannelGAN.

3) BLER Performance: To further prove the superiority of our proposed ChannelGAN, the link-level block error rate (BLER) performance comparison is presented in Fig. 6. Specifically, Real-SetA, Real-SetB and Real-SetC consist of 1000, 2000, and 20000 real channel samples, respectively. Fake-SetA and Fake-SetB indicate 20000 fake channel samples generated using ChannelGANs trained on Real-SetA and Real-SetB, respectively. Then, different EVCsiNet models are trained on different CSI sets from corresponding real or fake channel sets. Here we also provide the performance of codebook based scheme defined in 3GPP, namely eTypeII with feedback bits $B = 49$ [1]. It can be noticed that the EVCsiNets trained on Fake-SetA and Fake-SetB outperform the ones trained on Real-SetA and Real-SetB. Specifically, the performance of EVCsiNet trained on Fake-SetB almost approaches the upper bound trained on Real-SetC, which indicates that proposed ChannelGAN can significantly enhance the performance of DL-based CSI solutions with small set of real channel data, greatly reduces the demand for the amount of real channel data and further provides great potential of DL-based approaches for channel modeling and generating.

TABLE IV
FLOPS AND NUMBER OF TRAINABLE PARAMETERS COMPARISON

Structure	FLOPs ($\times 10^7$)	Trainable Par. ($\times 10^7$)
Generator G	3.493	1.747
Discriminator D	2.401	1.198

Note: The training time of 1200 epochs using $N_{\mathrm{s}} = 200$ real channel samples on a Tesla V100 32GB is about 13 minutes.

C. Complexity Analyses

The complexity of proposed ChannelGAN is described in Table IV from the perspective of floating point operations (FLOPs) and the number of trainable parameters.

V. CONCLUSION

In this letter, we propose a DL-based channel modeling and generating method refered to ChannelGAN, which is specifically designed on a small set of link-level MIMO channel defined in 3GPP. Moreover, two evaluation mechanisms including i) power comparison from the perspective of delay and antenna domain and ii) cross validation are implemented, where the power comparison proves the consistency between the modeled fake channel and real channel, and the cross validation verifies the effectiveness and availability of the generated fake channel for supporting related DL-based CSI feedback.

REFERENCES

[1] W. Liu, W. Tian, H. Xiao, S. Jin, X. Liu, and J. Shen, "EVCsiNet: Eigenvector-based CSI feedback under 3GPP link-level channels," *IEEE Wireless Commun. Lett.*, vol. 10, no. 12, pp. 2688–2692, Dec. 2021.
[2] H. Xiao *et al.*, "AI enlightens wireless communication: Analyses, solutions and opportunities on CSI feedback," *China Commun.*, vol. 18, no. 11, pp. 104–116, Nov. 2021.
[3] J. Wang, G. Gui, T. Ohtsuki, B. Adebisi, H. Gacanin, and H. Sari, "Compressive sampled CSI feedback method based on deep learning for FDD massive MIMO systems," *IEEE Trans. Commun.*, vol. 69, no. 9, pp. 5873–5885, Sep. 2021.
[4] J. Zeng, J. Sun, G. Gui, B. Adebisi, T. Ohtsuki, H. Gacanin, and H. Sari, "Downlink CSI feedback algorithm with deep transfer learning for FDD massive MIMO systems," *IEEE Trans. Cogn. Commun. Netw.*, vol. 7, no. 4, pp. 1253–1265, Dec. 2021.
[5] I. Goodfellow *et al.*, "Generative adversarial nets," in *Advances in Neural Information Processing Systems*, vol. 27. Red Hook, NY, USA: Curran, 2014.
[6] Y. Yang, Y. Li, W. Zhang, F. Qin, P. Zhu, and C.-X. Wang, "Generative-adversarial-network-based wireless channel modeling: Challenges and opportunities," *IEEE Commun. Mag.*, vol. 57, no. 3, pp. 22–27, Mar. 2019.
[7] S. Seyedsalehi, V. Pourahmadi, H. Sheikhzadeh, and A. H. G. Foumani, "Propagation channel modeling by deep learning techniques," 2019, *arXiv:1908.06767*.
[8] "Technical specification group radio access network; study on channel model for frequencies from 0.5 to 100 GHz (release 16)," 3GPP, Sophia Antipolis, France, Rep. TR 38.901 v16.1.0, 2020.
[9] I. Gulrajani, F. Ahmed, M. Arjovsky, V. Dumoulin, and A. Courville, "Improved training of Wasserstein GANs," 2017, *arXiv:1704.00028*.
[10] C. Villani, *Optimal Transport: Old and New*, vol. 338. Heidelberg, Germany: Springer, 2009.
[11] "Technical specification group radio access network; NR; physical layer procedures for data (release 16)," 3GPP, Sophia Antipolis, France, Rep. TR 38.214 v16.5.0, 2020.